applied optics

Ultralong focal length microlens array fabricated based on SU-8 photoresist

Rui Bian,[1] Ying Xiong,[1] Xiangyu Chen,[2] Penghui Xiong,[2] Shuangyue Hou,[1] Shan Chen,[1] Xiaobo Zhang,[1] Gang Liu,[1,*] and Yangchao Tian[1,3]

[1]National Synchrotron Radiation Laboratory, University of Science and Technology of China, Hefei 230029, China
[2]Department of Precision Machinery and Precision Instrumentation, University of Science and Technology of China, Hefei 230026, China
[3]e-mail: ychtian@ustc.edu.cn
*Corresponding author: liugang@ustc.edu.cn

Received 13 March 2015; revised 13 April 2015; accepted 5 May 2015; posted 6 May 2015 (Doc. ID 236129); published 28 May 2015

In this paper, a novel method to fabricate ultralong focal length microlens arrays has been proposed. The microlens arrays were fabricated based on surface tension when heating temperature is over a glass transition temperature of SU-8 photoresist. An ultralong focal length was achieved by the large radius of curvature of a photoresist surface. Microlenses of widths from 30 to 210 μm were successfully fabricated. The longest focal length was up to 4.4 mm from the microlens of 210 μm width. The formation mechanism was also studied and validated by simulation based on the finite element method.

OCIS codes: (220.0220) Optical design and fabrication; (220.4000) Microstructure fabrication; (160.5470) Polymers.

http://dx.doi.org/10.1364/AO.54.005088

1. INTRODUCTION

Microlens and microlens arrays (MLA) are widely used in the fields of imaging, integral photography, and atmospheric wavefront sensors known as Shack–Hartmann wavefront sensors (SHWS) [1]. Long focal length MLA is a vital optical element, which decides the performance of SHWS [2,3]. In recent years, many fabrication methods [4–8] were proposed to create a long focal length microlens or extend the focal length of MLA. The thermal reflow method has been proposed for many years [9,10]. The photoresist reflow method involves melting photoresist structures to fabricate a microlens shaped by the liquid resist's surface tension. This fabrication process is facile and cost effective. However, there were some potential drawbacks of the positive photoresist reflow method. It is difficult to achieve large focal length in the millimeter range for microlenses by positive photoresist thermal reflow process [11]. Besides, the profiles formed by this method could be much more complex than the simple surface energy minimization, which resulted in a huge aberration of the microlenses for certain fabrication parameters [9,10,12]. Hsieh *et al.* has presented a method to extend the focal length of reflowed microlens arrays based on two materials. By decreasing the refractive index difference between two layers of materials, the light rays could bend less when passing through MLA and could be focused on a farther distance [6]. Nevertheless, this process is complicated, and the quality of a microlens array relies on two materials. Difference of thermal expansion between the materials could cause thermal stresses, which could limit the application temperature range of the microlens arrays.

In order to achieve an ultralong focal length with small diameters of MLA, we proposed a novel method to fabricate the ultralong focal length MLA by a single kind of material. This is a facile and cost-effective fabrication approach. The ultralong focal length is determined by the large radius of curvature of a lens profile achieved due to surface tension. The longest focal length of MLA, which was fabricated and measured in experiment, could be up to 4.4 mm. To understand the formation mechanism of the microlens arrays, a finite element method (FEM) was studied using Surface Evolver software to simulate the forming process.

2. PRINCIPLE AND DESIGN

A diagram of the microlens array and light propagation path is shown in Fig. 1. Negative photoresist was used to fabricate microlens arrays. MLA structure was fabricated by the exposure process, and then a concave MLA was formed by heating the reflow procedure. Negative photoresist is typically low molecular weight polymer and exposed photoresist cross linked and formed high molecular weight polymer by chemical reaction [13]. In the following post-bake and reflow section, the exposed cross-linked polymer will not reflow, and the shape will stay unchanged. Meanwhile, unexposed resist will reflow to form a lens profile due to surface tension. Based on the negative photoresist microlens, a replication method was applied to translate the photoresist structure into the convex microlens.

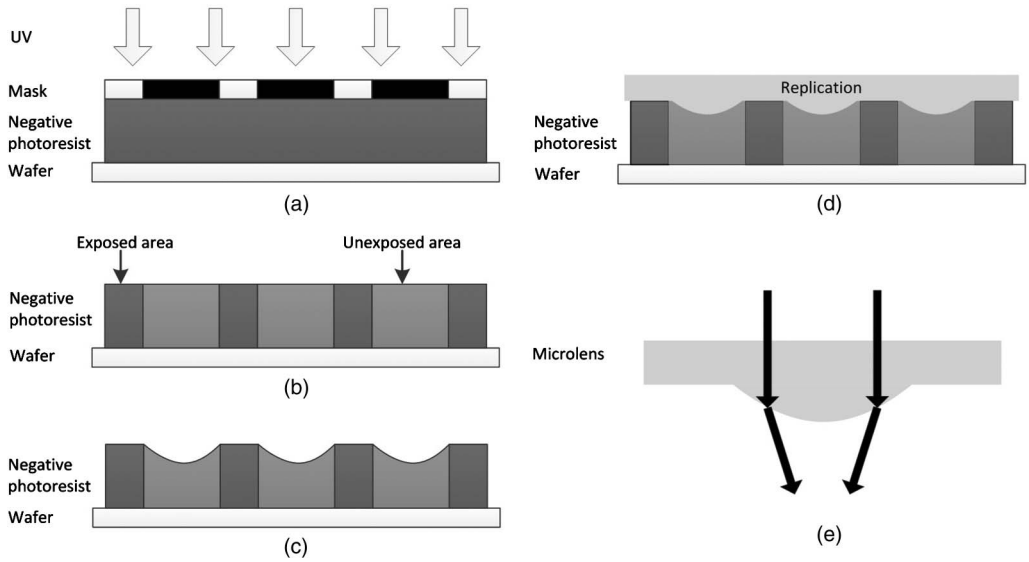

Fig. 1. Diagram of microlens array. Black arrows show the light propagation in a microlens. (a) Expose, (b) post exposure bake, (c) cooling, (d) PDMS molding, and (e) light propagation path in a microlens.

This microlens array is easy to test the optical performance. The focal length, f, of the convex microlens could be described as Eq. (1) and is shown in Fig. 1(e):

$$f = \frac{r_c}{n-1}, \tag{1}$$

where n is the refractive index of replicated microlens material and r_c is the radius of curvature. According to Eq. (1), the focal length is directly proportional to radius of the curvature instead of the thickness of photoresist. Long radius of curvature can be attained though rheological status during exposure and baking.

3. FABRICATION PROCESS AND EXPERIMENT

SU-8 photoresist was selected to fabricate ultralong focal length microlens arrays and PDMS was chosen as the replication material. The fabrication process is described and illustrated in Fig. 1. The Si wafer (127 mm × 127 mm × 0.5 mm) was rinsed with acetone and dried at 200°C for 30 min. The silicon wafer was then spin coated with a layer of 100 μm thick SU-8 photoresist (SU-8 2050, MicroChem) at 1700 rpm for 30 s and a two-step soft bake (65°C for 5 min and 95°C for 20 min) was performed on a level hot plate. The photoresist was then patterned with a photomask by UV exposure (i-line, 220 mJ/cm^2). A level hot plate was used for the post-exposure bake (PEB) (65°C for 5 min and 95°C for 10 min). After baking SU-8 photoresist, the substrate was allowed to cool down to ambient temperature on the hot plate to release stress. The PDMS was a two-part system with a mix ratio of cross-linker/curing agent A: siloxane $B = 1:10$. Upon mixing, the PDMS was degassed in a vacuum chamber. The appropriate PDMS was poured on photoresist. Placing the PDMS and photoresist in an oven at 50°C for 24 h cured the PDMS. After cooling to the ambient temperature, the PDMS mold can be easily detached from SU-8 microlens arrays without antistiction because of material property. Convex microlens arrays with large focal lengths were fabricated.

In order to obtain the morphology of various kinds of MLA, the diameters and widths of microlens arrays fabricated were from 30 to 390 μm, and the step length is 30 μm. The profiles of MLA were measured by surface profiler (XP-1 stylus Profiler, Ambios Technology), optical microscope, and scanning electron microscope (SEM).

4. RESULTS AND DISCUSSION

Microlenses with widths from 30 to 210 μm were successfully fabricated. The microscope image of microlens arrays and the scanning electron microscope (SEM) image of cross section of MLA are shown in Fig. 2. The width and contact angle of microlens are shown in this picture. In Fig. 2(a), the focused beam spots are in the center of each microlens. The spot profiles are symmetrical and have little variation, so the MLAs have high uniformity. In Fig. 2(b), the surface profile of the microlens is smooth and symmetrical, which means the microlens has good quality. In the widths from 30 to 390 μm, the 210 μm microlens was the biggest microlens demonstrated by this fabrication method, and it showed the longest focal length. For comparison, two sizes of MLA, 210 and 240 μm, were fabricated to illustrate the width effect. The surface profiles of microlenses with two widths measured by surface profiler are shown in Fig. 3. The dashed line is the profile of a microlens with 210 μm width. The dotted line shows the profile of a nonfully formed microlens with 240 μm width. The convex top profile is mainly caused by the large width, instead of insufficient bake time. In the large width, the viscosity of photoresist plays a big role in the formation process, so the effect of surface tension cannot reach to the center of microlens to form a complete arc.

A. Radius of Curvature and Contact Angles of MLA

The surface profile of a microlens is decided by the width and contact angle. The focal length of a microlens is determined by radius of the curvature. To achieve the surface profiles and to calculate the focal length of MLA, the morphology

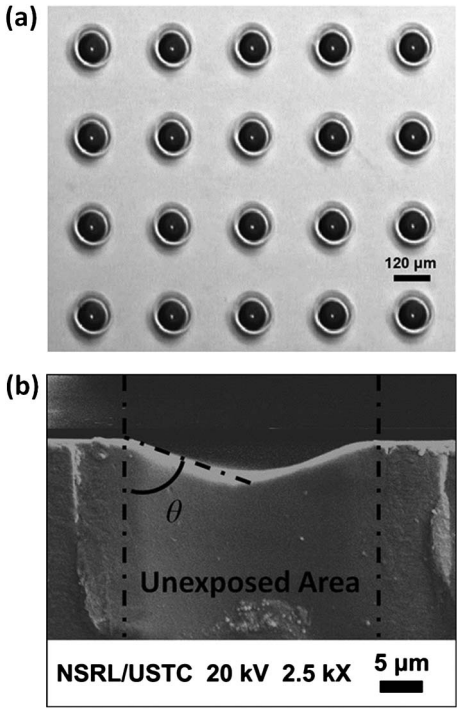

Fig. 2. (a) Microscope image of MLA. The focused beam spots are in the center of each microlens. (b) SEM image of cross section of a SU-8 microlens. The unexposed area is between the dashed lines, and the contact angle is indicated.

of MLA was measured by a surface profiler and scanning electron microscope.

Based on the data of morphology of the microlens, nonlinear curve fitting was applied to fit the surface profiles. Radius of the curvature was achieved from the fitting results. Figure 4 shows the radius of curvature of microlens arrays and the relational fitted curves of different widths. Based on the fitting result, the relation between radius of curvature and width is determined from Eq. (2):

$$r_c = 41.99 \times e^{\frac{w}{51.55}} - 87.36 \quad \textbf{(2)}$$

where r_c is the radius of curvature and w is the width of microlens. The Adj. R-Square (COD) shows the quality of a fit. The Adj. R-Square of radius fitting is 0.99, so the curve of microlens is well fitted, which means the result of the fitted radius is reliable. Results of radius could be used to calculate the focal length in the following section.

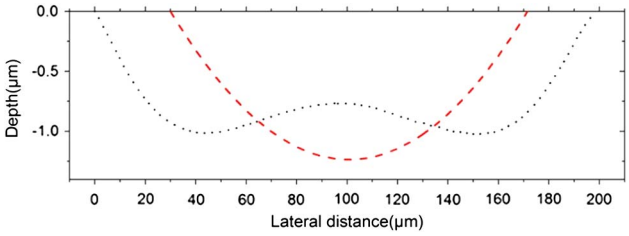

Fig. 3. Microlenses profiles by a surface profile. Dashed line is the profile of a microlens with 210 μm width. Dotted line shows the profile of a nonfully formed microlens with 240 μm width.

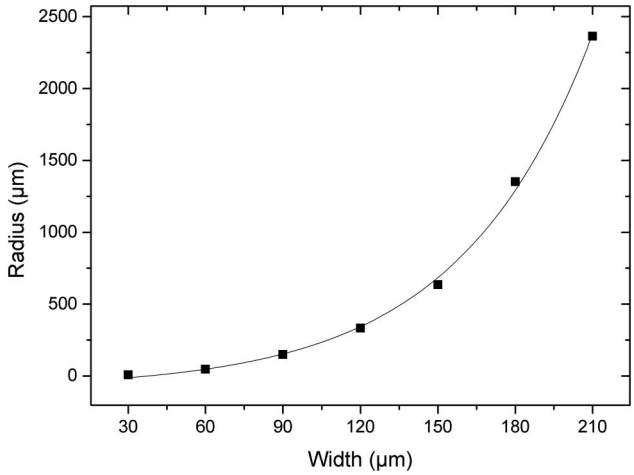

Fig. 4. Radius of microlenses and the curve fitting line. Square dots are the radius of curvature of microlenses, and widths of microlens are from 30 to 210 μm. Solid line is the curve fitting line.

In the ideal condition, the contact angle is decided by the solid, liquid, and vapor at a given temperature and pressure, instead of width of the microlens. In this condition, the contact angle is not affected by the width, and the radius is proportional to width of the microlens. The radius could be described as Eq. (3):

$$r_c = \frac{w}{2 \sin \theta}. \quad \textbf{(3)}$$

Compared with Eq. (2), Eq. (3) shows the exponential relationship between the radius and width. Based on the difference, it is expected that the contact angle of microlens changes with the width.

The contact angles of microlens arrays and the relational fitted curve of different widths are shown in Fig. 5, which shows the logarithmic relationship between the contact angles and width. According to the fitting result, the relation between contact angle and width is determined from Eq. (4):

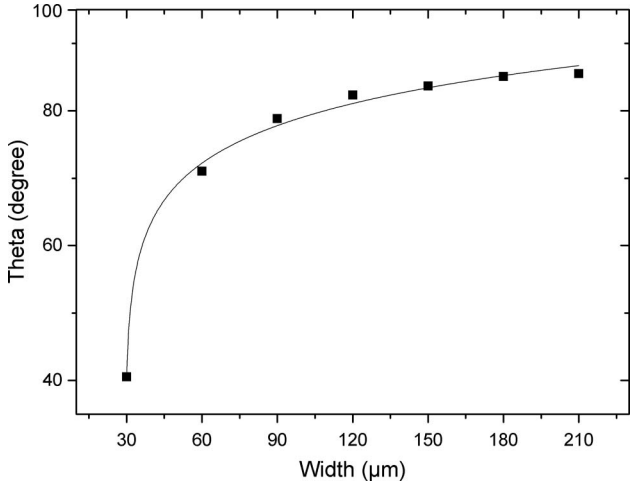

Fig. 5. Contact angles of microlenses and the curve fitting line. Square dots are the contact angles of microlenses and the widths of microlens are from 30 to 210 μm. Solid line is the curve fitting line.

$$\theta = 44.34 + 8.15 \times \ln(w - 29.37) \quad (4)$$

where θ is the contact angle and w is the microlens width.

When the microlens widths are below 90 μm, the contact angles increase significantly from 40 to 80 deg. It results in the radius of curvature enlarging slowly when the widths are below 90 μm. When the widths are above 90 μm, the contact angles increase slowly and approach 90 deg, finally, and the radius of curvature of MLA enlarges quickly. Therefore, the radius shows an exponential relationship with the width. The photoresist is polymer, and its viscosity is significant during the reflow process. The viscosity has a big effect on formation of a microlens, so the contact angle will change with the microlens width, which results in the nonlinear increase of radius.

To investigate the uniformity of the microlenses, standard deviation and relative standard deviation of radius are calculated in Table 1. The statistic results are based on 30 samples in each width. The RSD (relative standard deviation) is the standard deviation divide by average radius of curvature. The most RSD is below 5%, which means the uniformity of the fabricated lens is good. RSD of the microlens with the minimal (30 μm) and maximal (210 μm) width are bigger than the other's RSD. These larger deviations mean the trend of increasing and decreasing dimensions may be toward the fabrication process limit. Since the largest relative standard deviation is just 9.84%, this method is believed to provide good uniformity.

B. Focal Length of MLA

The focal length is relative directly to radius of the curvature of microlens arrays based on Eq. (1). According to Eqs. (1) and (2), the relation between the focal length and the width of microlens is determined by Eq. (5):

$$f = \frac{52.60 \times e^{\frac{w}{55.63}} - 115.67}{n - 1}, \quad (5)$$

where f is the focal length of the MLA, w is width of the microlens, and n is refractive index of the replicated microlens material. The equation could be used to calculate the focal length based on the data of morphology of a microlens measured in experiments.

A professional setup was implemented to measure the focal length of the microlens arrays and observe the optical quality.

Table 1. Results of Average Radius of Curvature[a]

Width (μm)	Average Radius of Curvature (μm)	Standard Deviation (μm)	Relative Standard Deviation (%)
30	8.44	0.70	8.29
60	46.07	1.52	3.29
90	148.89	8.90	5.97
120	333.11	16.40	4.92
150	635.55	31.16	4.90
180	1352.57	42.01	3.10
210	2364.78	232.71	9.84

[a]Standard deviation of radius and relative standard deviation of radius with widths from 30 to 210 μm.

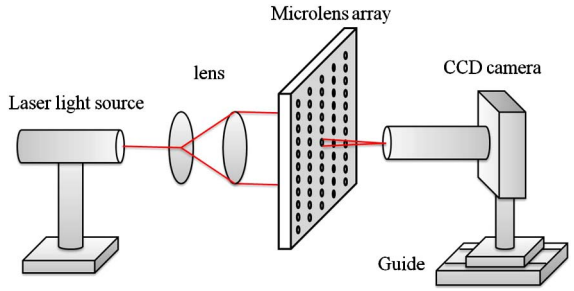

Fig. 6. Diagram of the setup to measure focal length of the MLA.

The setup [7] was composed of a 633 nm wavelength laser light source, a lens system, a CCD camera, a guide, and a computer, as shown in Fig. 6.

Result of the focal length based on the data of morphology of the microlens and measured by the optics setup is shown in Fig. 7. The square line is the focal length calculated based on the data of radius in experiments and Eq. (5). The dotted line is the focal length measured by the optics setup. The differences between the two kinds of values are slight in small widths. There are some differences in large widths, which could be caused by measurement error, fitting error, and spherical aberration. Based on the results of Fig. 7, the largest focal length is 4465 μm, which is much larger than that of a microlens fabricated by other methods [4–7]. The ultralong focal length is an advantage of this fabrication method.

In our experiment, the refractive index is $n = 1.41$ (PDMS). Based on the calculation of the previous section, the focal length is expected to be 2.43 times long as radius of the curvature. A longer focal length could be achieved by replacing the PDMS by other material with less refractive index.

C. Simulation of Microlens Arrays by FEM Software

To understand the formation mechanism of microlens arrays, a finite element method (FEM) was applied by Surface Evolver

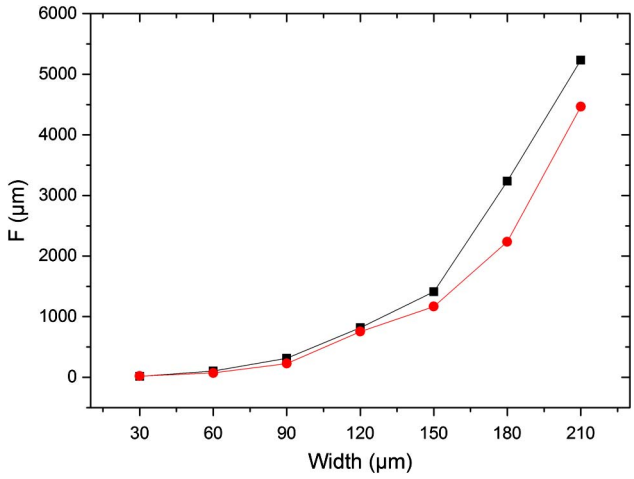

Fig. 7. Focal length of microlens arrays based on measurement of the morphology and optics performance. Square line is the focal length calculated based on the data of radius in experiment. Dotted line is the focal length measured by the optics setup.

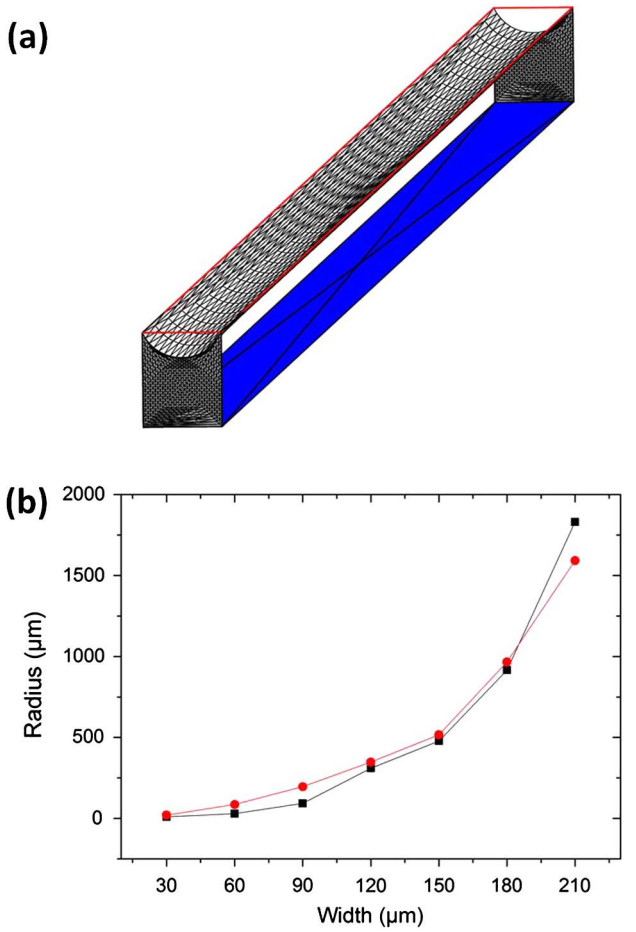

Fig. 8. (a) Model of simulation by Surface Evolver. (b) Radius of measured data and Surface Evolver simulations. Square line is the radius measured by the optics setup. Dotted line is the radius of curvature simulated by Surface Evolver.

software. When the unexposed photoresist was melted, the photoresist surfaces were pulled into a shape that minimizes the energy of the system due to the surface tension. If gravitational effects are presumed to be negligible, which, for very small lenses, will generally be the case, and assuming ideal conditions, one would expect the shape of these microlenses to be well approximated by a spherical surface [9,10]. In this simulation, we assumed the surface tension is the most important impact element. Surface Evolver is interactive software for the modeling of liquid surfaces shaped by various forces and constraints [14]. This finite-element-based software could be used to calculate the equilibrium shape of interfaces based on total energy minimization for defined surface tensions. A conjugate gradient method is applied to find the equilibrium state [15]. Given the geometry and contact angle, the software model could form the curved surface. Surface Evolver could cut the model into small pieces and do the iteration to minimize the energy. The model of simulation by Surface Evolver and the results of radius of the lens curvature simulated by Surface Evolver and measured by an optics setup are shown in Fig. 8. The square line is the radius measured by the optics setup. The dotted line is the radius of curvature simulated by Surface Evolver. The experimental result agrees well with the result of simulation, which proves the assumption that surface tension is the most crucial impact element of MLA's formation procedure is correct. It is concluded that the formation mechanism of a microlens is that the unexposed photoresist reflowed to form a spherical lens shape, which minimized the energy of surface due to surface tension. However, there were slight differences between the measured and simulated values. The reason of the deviation is that the reflowed SU-8 photoresist is rheological state, and there are other elements such as shrinkage of photoresist and viscosity to impact the formation process.

5. CONCLUSION

A new method to fabricate an ultralong focal length microlens has been proposed. Surface tension during post-baking was used to form the profile of the microlens. This fabrication approach is facile, cost-effective, highly reproducible, and easily controllable, offering a great opportunity for large-scale production of ultralong focal length microlens arrays. Various focal lengths have been achieved by regulating widths of the mask, in spite of photoresist thickness. The ultralong focal length, as long as 4.4 mm, was achieved in the experiment, which was much longer than that created by other methods. It is applicable in situations that require a long focal length such as wavefront detecting in Shack–Hartmann wavefront sensors. Ultralong focal length also provides large depth of focus, which can adopt position variance of an image sensor. Besides, it is useful for future photolithography technology.

The Major State Basic Research Development Program of China, Ministry of Science and Technology (2012CB825804).

REFERENCES

1. G. Artzner, "Microlens arrays for Shack–Hartmann wave-front sensors," Opt. Eng. **31**, 1311–1322 (1992).
2. G. Lelievre, J. Sebag, D. Bauduin, F. Fidouh, J. L. Lebrun, and B. Servan, "Wavefront sensors optimization in astronomical applications," Proc. SPIE **1781**, 224–231 (1993).
3. G. Y. Yoon, T. Jitsuno, M. Nakatsuka, and S. Nakai, "Shack Hartmann wave-front measurement with a large F-number plastic microlens array," Appl. Opt. **35**, 188–192 (1996).
4. F. Gex, D. Horville, G. Lelievre, and D. Mercier, "Improvement of a manufacturing technique for long focal length microlens arrays," Pure Appl. Opt. **5**, 863–872 (1996).
5. P. C. H. Poon, L. G. Commander, D. R. Selviah, and M. G. Robinson, "Extension of the useful focal length range of microlenses by oil immersion," J. Opt. A **1**, 133–141 (1999).
6. H.-T. Hsieh, V. Lin, J.-L. Hsieh, and G.-D. J. Su, "Design and fabrication of long focal length microlens arrays," Opt. Commun. **284**, 5225–5230 (2011).
7. L. Chen, S. Kirchberg, B. Y. Jiang, L. Xie, Y. L. Jia, and L. L. Sun, "Fabrication of long-focal-length plano-convex microlens array by combining the micro-milling and injection molding processes," Appl. Opt. **53**, 7369–7380 (2014).
8. Z. G. Zang, X. S. Tang, X. M. Liu, X. H. Lei, and W. M. Chen, "Fabrication of high quality and low cost microlenses on a glass substrate by direct printing technique," Appl. Opt. **53**, 7868–7871 (2014).
9. F. T. O'Neill and J. T. Sheridan, "Photoresist reflow method of microlens production part I: background and experiments," Optik **113**, 391–404 (2002).
10. F. T. O'Neill, C. R. Walsh, and J. T. Sheridan, "Photoresist reflow method of microlens production: modeling and fabrication

techniques," in *Photon Management*, F. Wyrowski, ed. (SPIE, 2004), pp. 197–208.
11. H. Ottevaere, R. Cox, H. P. Herzig, T. Miyashita, K. Naessens, M. Taghizadeh, R. Volkel, H. J. Woo, and H. Thienpont, "Comparing glass and plastic refractive microlenses fabricated with different technologies," J. Opt. A **8**, S407–S429 (2006).
12. A. Schilling, R. Merz, C. Ossmann, and H. P. Herzig, "Surface profiles of reflow microlenses under the influence of surface tension and gravity," Opt. Eng. **39**, 2171–2176 (2000).
13. H. Lorenz, M. Despont, N. Fahrni, N. LaBianca, P. Renaud, and P. Vettiger, "SU-8: a low-cost negative resist for MEMS," J. Micromech. Microeng. **7**, 121–124 (1997).
14. K. A. Brakke, "The surface evolver and the stability of liquid surfaces," Philos. Trans. R. Soc. A **354**, 2143–2157 (1996).
15. S. F. Chini and A. Amirfazli, "Understanding pattern collapse in photolithography process due to capillary forces," Langmuir **26**, 13707–13714 (2010).